Autoantibody-induced internalization of CNS AQP4 water channel and EAAT2 glutamate transporter requires astrocytic Fc receptor

Shannon R. Hinson[a], Ian C. Clift[a,1], Ningling Luo[a], Thomas J. Kryzer[a], and Vanda A. Lennon[a,b,c,2]

[a]Neuroimmunology Laboratory, Department of Laboratory Medicine and Pathology, College of Medicine, Mayo Clinic, Rochester, MN 55905; [b]Department of Neurology, College of Medicine, Mayo Clinic, Rochester, MN 55905; and [c]Department of Immunology, College of Medicine, Mayo Clinic, Rochester, MN 55905

Edited by Peter Agre, Johns Hopkins Bloomberg School of Public Health, Baltimore, MD, and approved April 10, 2017 (received for review February 10, 2017)

Aquaporin-4 (AQP4) water channel-specific IgG distinguishes neuromyelitis optica (NMO) from multiple sclerosis and causes characteristic immunopathology in which central nervous system (CNS) demyelination is secondary. Early events initiating the pathophysiological outcomes of IgG binding to astrocytic AQP4 are poorly understood. CNS lesions reflect events documented in vitro following IgG interaction with AQP4: AQP4 internalization, attenuated glutamate uptake, intramyelinic edema, interleukin-6 release, complement activation, inflammatory cell recruitment, and demyelination. Here, we demonstrate that AQP4 internalization requires AQP4-bound IgG to engage an astrocytic Fcγ receptor (FcγR). IgG-lacking Fc redistributes AQP4 within the plasma membrane and induces interleukin-6 release. However, AQP4 endocytosis requires an activating FcγR's gamma subunit and involves astrocytic membrane loss of an inhibitory FcγR, CD32B. Interaction of the IgG–AQP4 complex with FcγRs triggers coendocytosis of the excitatory amino acid transporter 2 (EAAT2). Requirement of FcγR engagement for internalization of two astrocytic membrane proteins critical to CNS homeostasis identifies a complement-independent, upstream target for potential early therapeutic intervention in NMO.

neuromyelitis optica | CD32 | CD64 | pathogenic IgG | autoimmune astrocytopathy

Neuromyelitis optica (NMO) is a relapsing inflammatory autoimmune demyelinating disease of the central nervous system (CNS), long considered a severe form of multiple sclerosis (MS). Attacks are generally more severe, onset of paralysis and blindness more rapid (1), and standard MS therapies can worsen NMO (2, 3). A specific serum IgG allows early distinction from MS, thus ensuring timely appropriate therapy (4, 5).

The aquaporin-4 (AQP4) water channel is the CNS target (4). Outcomes documented in vitro after NMO-IgG binds to the AQP4 extracellular domain on astrocytes include AQP4 endocytosis and lysosomal degradation, loss of its physically linked major excitatory amino acid transporter 2 (EAAT2), reduced glutamate uptake, impaired water fluxes, granulocyte chemotaxis, and complement factor transcription, secretion, and activation (1, 6–11). Ensuing endothelial permeation of circulating immunoglobulins, complement components, and leukocytes magnifies the initial inflammatory response (6–12). Immunopathological analyses of NMO patients' CNS tissues attest to these events occurring in vivo and inform lesional evolution at the target astrocyte level (1). The blood–brain barrier (BBB) does not absolutely restrict IgG entry into the CNS, but it does exclude macromolecular C1q, essential for activating the classical complement cascade.

Experimental studies of lesional events in vitro and in animal models of NMO have emphasized complement-mediated inflammation and astrocyte cytolysis, late events associated with extensive BBB disruption. A neglected potential initiator of NMO pathophysiology is the AQP4-IgG–activated astrocyte's response: synthesis and secretion of complement, cytokines, chemokines (12–14), and inflammatory mediators attracting NMO-characteristic granulocytes. Focally enhanced BBB permeability (7, 12) plausibly accounts for initially reversible early NMO symptoms and MRI abnormalities. Early lesions contain viable, phenotypically activated astrocytes lacking AQP4 and EAAT2 (6, 15), with myelin intact but focally edematous (9).

Here, we report that internalization of AQP4 and its linked EAAT2 glutamate transporter requires AQP4-specific IgG to engage both AQP4 and an astrocytic Fc gamma receptor (FcγR). We additionally show that AQP4 clustering and initiation of astrocytic IL-6 release by IgG are independent of Fc receptor signaling. Delineation of these pathways may identify upstream targets for selective therapeutic attenuation of NMO evolution.

Results

AQP4 Internalization by NMO-IgG Is Fc-Dependent. We previously demonstrated that NMO-IgG binding to AQP4 in live cells causes membrane AQP4 to relocate to the endolysosomal path (6, 9, 10). To separate early events from downstream Fc-dependent events, we investigated $F(ab')_2$ prepared from NMO patients and healthy subjects. Like serum and IgG, NMO-$F(ab')_2$ bound at 4 °C to live astrocytes (Fig. 1*A*). Western blot revealed that plasma membrane AQP4 was reduced more than fivefold in astrocytes exposed, at 37 °C, to NMO serum or IgG, or an AQP4 extracellular domain-specific mouse monoclonal IgG (mECD), by comparison with membranes exposed to control serum, IgG or an AQP4

Significance

Neuromyelitis optica (NMO) is a severe inflammatory central nervous system demyelinating disease (IDD). Detection of NMO-specific IgG in serum distinguishes NMO from other IDDs, enables rapid diagnosis, and expedites NMO-appropriate therapy. Binding of NMO-IgG to aquaporin-4 (AQP4), the astrocytic water channel antigen, initiates endocytosis of AQP4 and its coupled EAAT2 glutamate transporter. Sequelae potentially contributing to NMO lesions include reduced water fluxes, reduced extracellular glutamate clearance, activation of a proinflammatory astrocyte response, and complement activation. Our paper investigates early events following IgG–AQP4 interaction and demonstrates that AQP4 and EAAT2 internalization, but not astrocytic secretion of IL-6, requires astrocytic Fc receptor signaling. Selective attenuation of these signaling events offers an upstream therapeutic target.

Author contributions: S.R.H., I.C.C., and V.A.L. designed research; S.R.H., I.C.C., and N.L. performed research; T.J.K. contributed new reagents/analytic tools; S.R.H. and V.A.L. analyzed data; and S.R.H. and V.A.L. wrote the paper.

Conflict of interest statement: V.A.L. and T.J.K. are named inventors on a patent relating to AQP4 as NMO antigen, but receive no royalties from service tests performed by Mayo Medical Laboratories. Earnings from technology licensing have exceeded the federal threshold for significant interest. V.A.L. and S.R.H. are named inventors on two patent applications filed by Mayo Foundation relating to functional clinical assays for detecting AQP4-IgG.

This article is a PNAS Direct Submission.

Freely available online through the PNAS open access option.

[1]Present address: School of Applied Health Sciences, Dwyer College of Health Sciences, Indiana University, South Bend, IN 46634.

[2]To whom correspondence should be addressed. Email: lennon.vanda@mayo.edu.

This article contains supporting information online at www.pnas.org/lookup/suppl/doi:10.1073/pnas.1701960114/-/DCSupplemental.

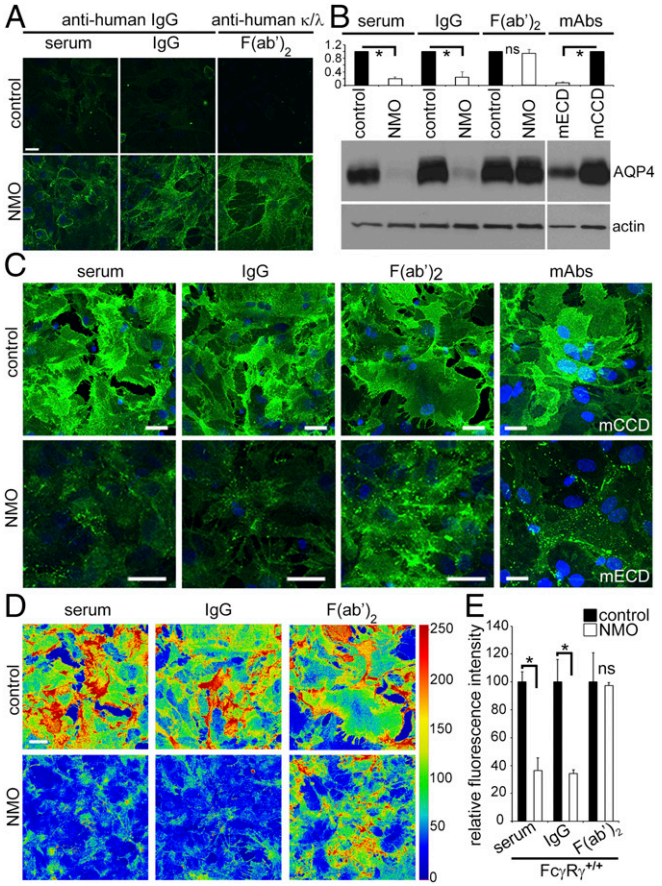

Fig. 1. NMO-IgG Fc-domain is required for AQP4 internalization. (*A*) Immunofluorescence: Human IgG bound to live astrocytes after 4 °C exposure to IgG products. Only NMO products bound (green). (*B*) Western blot: AQP4 in membranes of astrocytes exposed to human IgG or monoclonal IgGs (normalized to actin). NMO serum or IgG, or mAb mECD, reduced AQP4 ($*P < 10^{-7}$; NMO compared with control patient specimens; $*P < 10^{-6}$; mECD compared with mAb mCCD. F(ab′)$_2$ did not reduce AQP4 ($P = 0.164$). (*C*) AQP4 distribution did not change after exposure to control patient preparations or mCCD mAb. NMO preparations and mAb mECD, reduced AQP4; NMO-F(ab′)$_2$ redistributed but did not reduce AQP4. DNA, blue (DAPI). (*D*) AQP4 immunofluorescence intensity in thermal LUT (look up table) images of *C* raw images. (*E*) AQP4 quantified from *C* images. Error bars: SD of the mean, three or more images per condition [$*P < 0.0002$ (serum) and 0.002 (IgG); ns, not significant]. (Scale bars: *A*, 20 μm; *C*, 20 μm; *D*, arbitrary units.)

cytoplasmic C-terminal-specific mAb IgG (mCCD) (Fig. 1*B*). NMO-F(ab′)$_2$ exposure did not change the membrane AQP4 content (Fig. 1*B*), suggesting that the Fc domain is necessary to trigger AQP4 removal. We therefore examined astrocytes exposed to NMO serum, IgG, or F(ab′)$_2$ at 37 °C. All three preparations redistributed AQP4 into membrane puncta (Fig. 1*C*). NMO serum and IgG reduced AQP4 compared with control serum and IgG (Fig. 1 *C*–*E*). Similar to NMO-IgG, mECD induced AQP4 clustering and internalization (Fig. 1*C*); mCCD did not redistribute AQP4 (Fig. 1*C*). NMO-F(ab′)$_2$ induced puncta formation but did not reduce AQP4 staining intensity (Fig. 1 *C*–*E*). Thus, despite redistributing AQP4 in the membrane, NMO-F(ab′)$_2$ did not cause internalization.

Dual AQP4 and early endosome antigen 1 (EEA1) staining confirmed that AQP4 cross-linked by NMO-F(ab′)$_2$ does not enter the endolysosomal pathway. AQP4 and EEA1 colocalization was observed after exposure to NMO serum or IgG (Fig. 2*A*; arrows), but not NMO-F(ab′)$_2$ or control products ($n > 100$; Fig. 2*A*). A lysosome-associated membrane glycoprotein 1 (LAMP-1) probe verified that NMO-IgG–induced AQP4-EEA1 clusters were destined for degradation (Fig. 2*B*). The results suggest AQP4 degradation requires AQP4-bound IgG to interact with an FcγR.

AQP4 Internalization by NMO-IgG Involves FcγRs. To further investigate AQP4 persistence in astrocytic membranes despite cross-linking by NMO-F(ab′)$_2$ (Fig. 1), we tested IgG and F(ab′)$_2$ effects on astrocytes from mice lacking the gamma subunit common to activating Fcγ receptors [FcγRI, FcγRIII, and FcεRI (*Fcer1g*^{tm1Rav})]. Gamma is required for the ITAM signaling response when IgG binds to the alpha subunit (16). Membrane AQP4 distribution was unchanged in FcγRγ$^{-/-}$ astrocytes exposed to control serum, IgG, or F(ab′)$_2$ (Fig. 3*A*), but NMO serum, IgG, and F(ab′)$_2$ induced AQP4 clusters indistinguishable from those induced on FcγR$^{+/+}$ astrocytes. Both NMO serum and IgG reduced the FcγR$^{+/+}$ astrocytes' AQP4 fluorescence intensity (Fig. 3*B*), but neither NMO serum nor IgG reduced FcγRγ$^{-/-}$ astrocytes' AQP4 fluorescence intensity, despite AQP4 aggregation (Fig. 3*B*). NMO-F(ab′)$_2$ did not reduce either FcγR$^{+/+}$ or FcγRγ$^{-/-}$ astrocytes' AQP4 intensity (Fig. 3*B*). By Western blot, AQP4 was not reduced in FcγRγ$^{-/-}$ astrocytes exposed to IgG or F(ab′)$_2$, or mouse mAbs (Fig. 3*C*). In contrast, FcγR$^{+/+}$ astrocytes exposed to NMO-IgG lost more than 70% AQP4 (Fig. 3*C*).

We next investigated whether interleukin-6 (IL-6) release, another known outcome of NMO-IgG binding (13, 14), also is FcγR-dependent. IL-6 secretion did not increase from wild-type or FcγRγ$^{-/-}$astrocytes exposed to control serum, IgG, or F(ab′)$_2$, but both released IL-6 after 4 h exposure to NMO serum, IgG, or F(ab′)$_2$ (Fig. 3*D*). The IL-6 concentration increased further after 6 and 8 h. Wild-type and FcγRγ$^{-/-}$ astrocytes released similar amounts of IL-6 after exposure to NMO serum, IgG, or F(ab′)$_2$. We conclude that IL-6 secretion induced by NMO-IgG does not require AQP4 internalization, the NMO-IgG Fc domain, or an FcγR gamma subunit.

Microglia Not Required for NMO-IgG To Initiate AQP4 Redistribution or Degradation. Primary glial cultures express FcγRs on astrocytes (~95% of cells) and microglia (<5%) (17–20), but only astrocytes express AQP4. To identify the FcγR-expressing cell type initiating AQP4 translocation to the astrocytic endolysosomal path following NMO–IgG interaction, we eliminated microglia with liposomal clodronate (Clodrosome). Dual immunostaining of the microglial ionized calcium binding adaptor 1 (Iba-1) and the astrocytic cytoskeletal intermediate filament, glial fibrillary acidic protein (GFAP), confirmed microglial depletion (Fig. 4*A*). AQP4 redistribution by NMO-IgG did not require microglia. In their absence, exposure to NMO serum, IgG, F(ab′)$_2$, or mECD caused AQP4 redistribution (Fig. 4*B*), but exposure to control-IgG and mCCD preparations did not. Western blot of astrocytic membranes confirmed that microglial depletion did not affect AQP4 loss (Fig. 4 *C* and *D*). Because NMO-IgG–induced AQP4 degradation did not require microglial FcγR engagement, we concluded that AQP4 endocytosis and degradation involves AQP4-bound IgG interaction with an astrocytic FcγR.

Astrocytic EAAT2 Glutamate Transporter Degradation Requires FcγR Engagement by AQP4-Complexed IgG. Extracellular glutamate clearance is a critical function of astrocytes embracing glutamatergic synapses. By removing 90% of exocytosed glutamate, EAAT2 prevents glutamate toxicity in the course of excitatory CNS neurotransmission. EAAT2 loss is a striking feature of early, non-destructive spinal gray matter lesions in autopsied NMO patients (6). Furthermore, live astrocytes exposed in vitro to NMO-IgG transport less glutamate (6, 11, 21) because, being noncovalently linked to AQP4, EAAT2 is coendocytosed (6). We therefore evaluated NMO-F(ab′)$_2$ effect on EAAT2. In contrast to NMO serum causing 50% loss of membrane EAAT2 (Fig. 4 *E* and *F*), NMO-F(ab′)$_2$ did not reduce EAAT2 (Fig. 4 *E* and *F*). We conclude that the NMO-IgG Fc domain is required for EAAT2 cointernalization with AQP4.

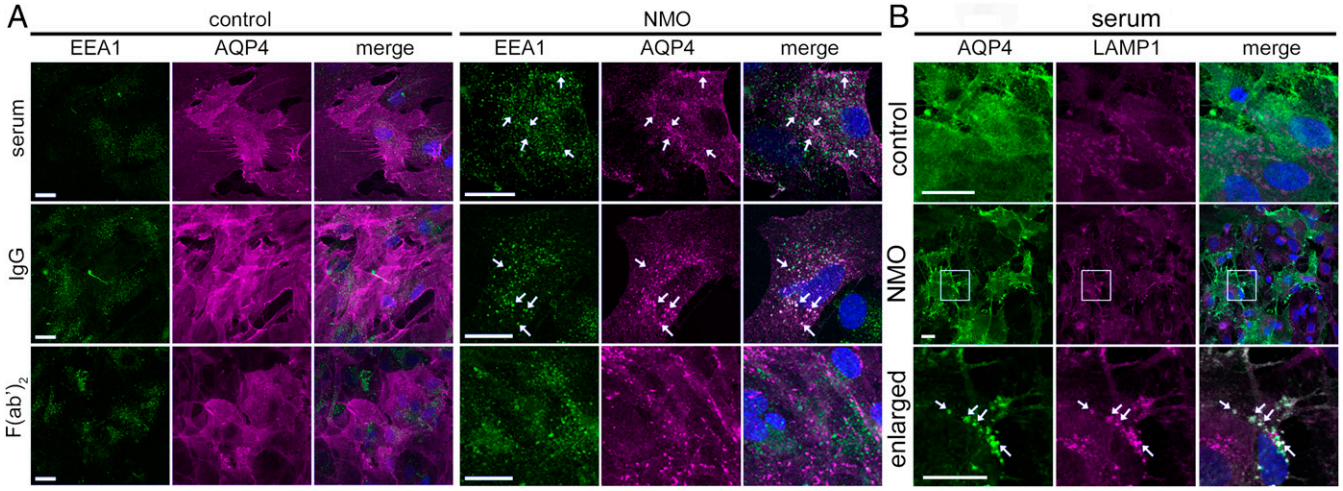

Fig. 2. NMO-IgG Fc domain is required for astrocytic lysosomal degradation of AQP4. (*A*) After exposure to control or NMO patient products. AQP4, magenta; early endosome marker (EEA1), green. Arrows, AQP4 entering endosomal degradative path (merged is white). (*B*) AQP4 (green) colocalizes with lysosomal LAMP-1 (magenta) after exposure to NMO but not control serum. (Scale bars: 20 μm.)

NMO-IgG Binding to AQP4 Triggers Inhibitory CD32B FcγR Loss from Astrocytic Membranes. Because our results implicate FcγR signaling in NMO-IgG–induced endocytosis of AQP4 and EAAT2, we imaged FcγRs in cultured astrocytes (Fig. 5*A*): CD64 (activating FcγRI) was in cytoplasm and membranes. CD32B (inhibitory FcγRIIB) surrounded nuclei and coincided with AQP4 in membrane patches (arrows, Fig. 5*A*, *Inset*). CD16 (activating FcγRIII) was not detected. Western blots confirmed CD64 in lysates, regardless of serum exposure (*SI Results* and Fig. S1). CD16 and CD32B were not detected, but were abundant in control spleen (Fig. S1). Immunoprecipitation enriched CD32B at every time point examined, regardless of serum exposure (Fig. 5*B*).

We next investigated astrocytic CD32B localization in relation to AQP4. Control serum exposure (6 h) did not change CD32B or AQP4 distribution (Fig. 5*C*), but NMO serum caused AQP4 and CD32B coaggregation into puncta. Exposure to mECD (but not to mCCD) also caused CD32B-AQP4 coaggregation (Fig. 5*D*). Thus, we attributed the NMO serum effect on CD32B localization to AQP4-specific IgG and not to a putative CD32B-reactive IgG.

We measured membrane FcγR changes after serum or IgG incubation by interval flow cytometry, with probe IgGs: CD32B, CD64, AQP4 extracellular domain, and GFAP (fixed and permeabilized). The geometric mean AQP4-IgG fluorescence on AQP4-null astrocytes (nonspecific) was subtracted from all AQP4 values. Compared with control serum or IgG, membranes lost ∼50% AQP4 after 16 h of NMO serum or IgG exposure (Fig. 6*A*). CD64 fluorescence after control or NMO serum exposure trended downward, compared with nonexposed astrocytes, but differences were not significant (Fig. 6*B*), suggesting a nonspecific effect. CD32B also trended downward after serum exposure (Fig. 6*C*). Compared with nonexposed astrocytes, NMO serum induced significant CD32B loss at 2 and 16 h (Fig. 6*C*); control serum reduced CD32B at 16 h (Fig. 6*C*). At 2 h, CD32B loss was greater with NMO serum than control serum. The results suggest a targeted removal of CD32B from the plasma membrane by NMO serum.

To differentiate nonspecific serum or IgG effects on Fc receptors, we compared expression levels of AQP4, CD64, and CD32B on astrocytes exposed to control or NMO serum. AQP4 increased transiently after 30 min with NMO serum (Fig. 6*D*), presumably reflecting surface coalescence of AQP4 cross-linked by NMO-IgG. Membrane loss of AQP4 was evident within 2 h of NMO serum exposure and was sustained at 16 h (Fig. 6*D*). CD64 did not change appreciably at any time point with control or NMO serum (Fig. 6*E*). CD32B was unchanged after 30 min with either serum, but was reduced significantly after 2 h with NMO serum (Fig. 6*F*), and remained significantly reduced after 16 h (Fig. 6*F*). Thus, partial CD32B internalization accompanies AQP4 endocytosis after IgG binds.

Internalization of both CD32B and AQP4 Requires FcγR Gamma Subunit. Surface CD64 did not change detectably on wild-type astrocytes exposed to NMO-IgG (Fig. 6*E*), but astrocytes lacking the gamma subunit (FcγRγ$^{-/-}$) failed to endocytose AQP4 (Fig. 3*C*). Endocytosis of the IgG:AQP4:CD32B complex appears to require signaling through CD64. We compared AQP4, CD64, and CD32B expression on serum-exposed FcγRγ$^{-/-}$ astrocytes. Interval FACS analyses showed no AQP4 loss from FcγRγ$^{-/-}$ membranes after NMO serum exposure (Fig. 6*G*). CD64 alpha subunit increased modestly after 30 min, but returned to baseline at 2 h and 16 h (Fig. 6*H*). Surface CD32B on FcγRγ$^{-/-}$ astrocytes did not change after 2 h of exposure to NMO serum (Fig. 6*I*).

We demonstrated that IgG is the NMO serum component responsible for astrocytic CD32B loss by exposing wild-type and FcγRγ$^{-/-}$ astrocytes for 2 h to IgG purified from control or NMO patient serum. Only NMO-IgG caused CD32B loss from wild-type astrocytes (Fig. 6*J*). Neither IgG affected CD32B expression on FcγRγ$^{-/-}$ astrocytes (Fig. 6*J*), despite CD64 alpha subunit presence (Fig. 6*K*). Our results demonstrate that NMO–IgG–AQP4 interaction causes endocytosis of AQP4 and CD32B and that this outcome involves an astrocytic FcγR gamma subunit.

CD32B Phosphorylation Follows NMO-IgG Binding to AQP4 on the Astrocyte Plasma Membrane, and Precedes Loss of AQP4 and CD32B. Leukocyte studies demonstrated that IgG cross-linking of FcγRs is followed by CD32B phosphorylation and subsequent endocytosis (22). We analyzed the phosphorylation state of CD32B immunoprecipitated from lysates of serum-exposed astrocytes by probing duplicate Western blots for CD32B and phosphorylated CD32B (pCD32B). By comparison with cells exposed to control serum, pCD32B approximately doubled after 2 min of exposure to NMO serum (Fig. 7 *A* and *B*) or IgG (Fig. 7 *C* and *D*), and was greatest at 10 min. As observed on nontreated astrocytes (Fig. 5*C*), total CD32B was low on astrocytes exposed to control or NMO-F(ab′)$_2$ for 2–10 min (Fig. 7*E*). Our results show that after NMO-IgG binds to AQP4, endocytosis is preceded by an increase and phosphorylation of membrane CD32B.

Discussion

Investigation of central nervous system FcγRs has been limited to date. Our observations assign a role to astrocytic FcγRs, by identifying their signaling as an upstream event in NMO pathogenesis. Astrocytic FcγR involvement in autoantibody-initiated

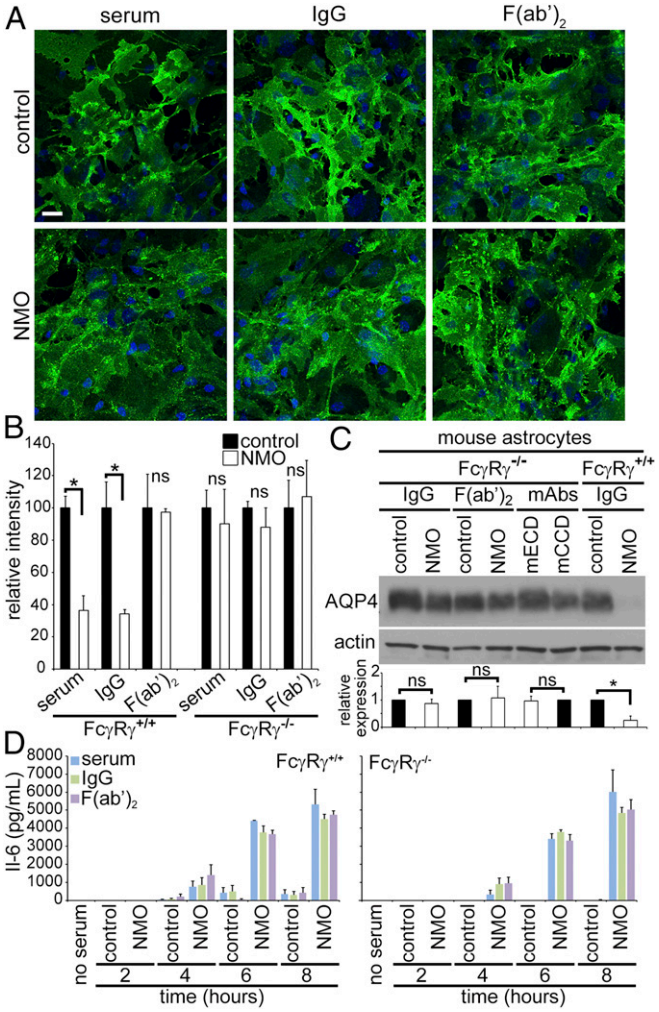

Fig. 3. Astrocytic FcγR engagement is required for AQP4 internalization by NMO-IgG, but not for AQP4 clustering. (*A*) AQP4 (green) in membranes of astrocytes from $Fc\gamma R\gamma^{-/-}$ mice remains diffusely distributed after exposure to control serum, IgG or $F(ab')_2$, but is clustered after exposure to NMO serum, IgG, or $F(ab')_2$. DNA, blue (DAPI). (*B*) AQP4 quantified on $Fc\gamma R^{+/+}$ and $Fc\gamma R\gamma^{-/-}$ astrocytes after exposure to control or NMO patients' products. Error bars: SD of the mean, three or more images per condition [$*P < 0.0002$ (serum) and 0.002 (IgG); ns, not significant]. (*C*) Membrane AQP4 from astrocytes exposed to control or NMO-IgG or $F(ab')_2$ or mouse mAbs. AQP4 is retained in membranes lacking FcγR gamma, but lost from wild-type membranes ($*P < 10^{-4}$). (*D*) Regardless of FcγRγ status, IL-6 is detectable in astrocyte media within 4 h of exposure to NMO serum, IgG, or $F(ab')_2$, but not to control serum or Ig products.

internalization of both AQP4 and EAAT2 is unprecedented. Our further demonstration that astrocytes exposed to NMO-$F(ab')_2$ release IL-6, without internalizing AQP4, is consistent with the documented proinflammatory response stimulated in astrocytes as an outcome of AQP4 clustering: secretion of complement components, chemokines, and cytokines (13, 14). IL-6 is a critical mediator of CNS inflammation in NMO (23, 24), as evidenced by the therapeutic benefit of monoclonal IgG blockade of IL-6 (25). *Ex vivo*, IL-6 released by astrocytes exposed to NMO-IgG reduced CNS capillary endothelial barrier function, increased CCL2 and CXCL8 production, and promoted leukocyte transmigration under flow conditions; these effects were neutralized by IL-6–specific IgG (12). Transient removal of the CD32B inhibitory receptor from astrocyte surfaces in the course of NMO-IgG–induced FcγR signaling might enhance IL-6 release. Selective CD32B blockade in human monocytes triggers release of IL-6 and other cytokines and chemokines (26).

Investigation of these events in an animal model is beyond the scope of our study. Most NMO models reported to date recapitulate late complement-mediated, tissue destructive events and require CNS lesioning to allow access of circulating AQP4-specific IgG and complement. A newly described rat model, induced by chronic intrathecal AQP4-IgG infusion (27), recapitulates early events, including reversible motor paresis, NMO-typical MRI lesions, loss of both AQP4 and EAAT2, and preserved myelin and astrocyte integrity. Our study investigates signaling events initiated within minutes of NMO-IgG binding to AQP4.

Many FcγR functions documented in immunocytes require recruitment of additional Fc-binding molecules by IgG bound via its

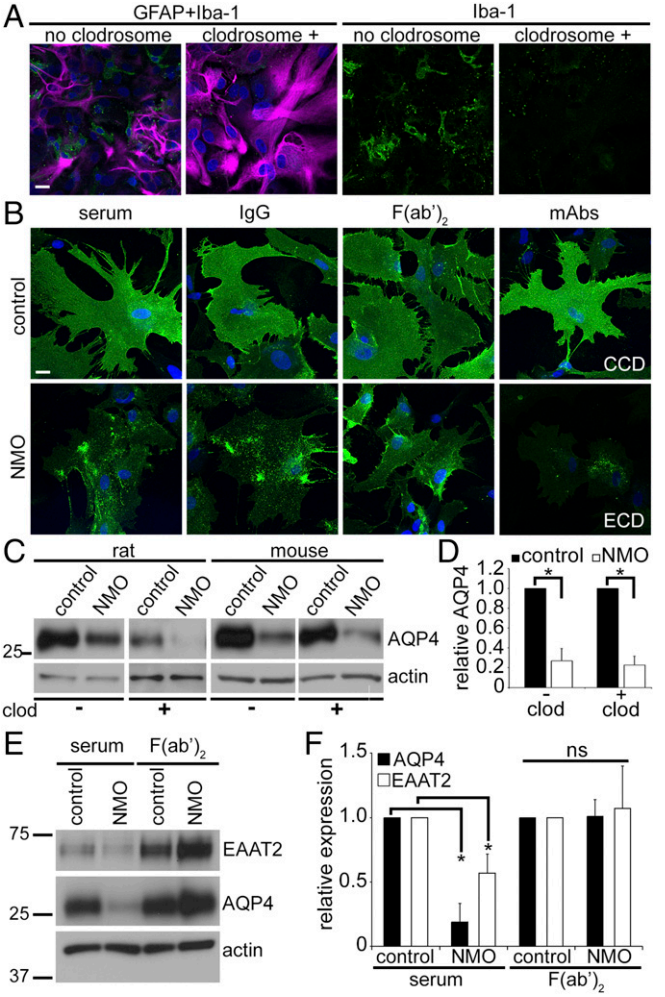

Fig. 4. Microglia are not required for astrocytic AQP4 internalization. (*A*) Clodrosome depletes microglial colonies (green, Iba-1^+) in mixed cultures (magenta, $GFAP^+$ astrocytes). (*B*) Distribution of AQP4 (green) in cultures lacking microglia was not affected by control serum, IgG or $F(ab')_2$, or mCCD. NMO serum, IgG, and mECD induced AQP4 redistribution and loss; NMO-$F(ab')_2$ induced AQP4 redistribution, but not loss. DNA, blue (DAPI). (Scale bars: 20 μm.) (*C*) Western blot analysis of AQP4 in rat and mouse astrocytes exposed to control or NMO-IgG in presence and absence of microglia (- or + clodrosome). (*D*) Membrane AQP4 content (normalized to actin) reduced equivalently by NMO-IgG exposure, relative to control-IgG-exposure, regardless of microglial presence (- clod, + clod); $*P < 10^{-5}$. (*E*) Western analysis of mouse astrocyte membranes exposed to control or NMO serum, or $F(ab')_2$. Blots probed for EAAT2, AQP4, and actin. (*F*) Quantitation of autoradiograms (three independent experiments); $*P < 10^{-5}$ (AQP4) and $P < 0.008$ (EAAT2). ns, not significant.

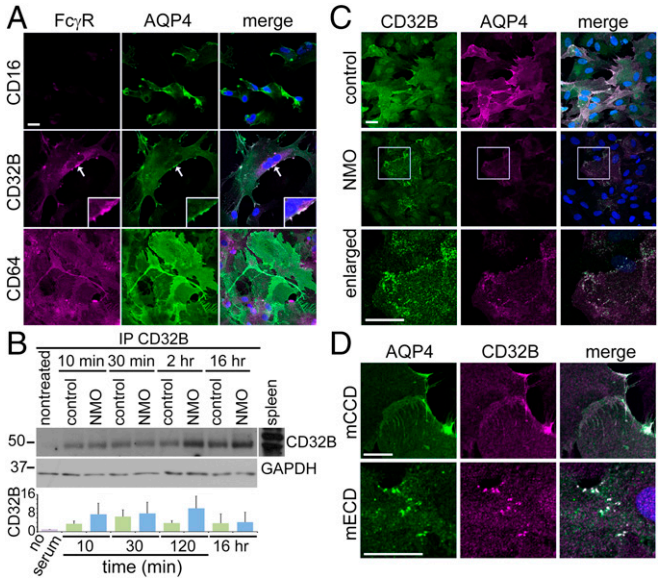

Fig. 5. CD32B and CD64 FcγRs in rat astrocyte membranes before and after human serum exposure. (*A*) Basal FcγR immunostaining (magenta). CD16 is undetectable. CD32B is enriched on the membrane (arrow and *Inset*) and around the nucleus. AQP4 (green) colocalizes with CD32B (merged, white). CD64 distribution is uniform on plasma membranes. Small CD64$^+$ cells are presumed microglia. (*B*) Western blotted CD32B precipitated by CD32B-IgG from astrocytes lysed after human serum exposure (GAPDH indicates relative protein load). Bar graph shows no significant difference in CD32B immunoreactivity precipitated after either serum exposure (control, green; NMO, blue). (*C*) CD32B (green) and AQP4 (magenta) are distributed uniformly after exposure to control serum (merged, white); after NMO serum exposure, they cluster in foci (shown enlarged). (*D*) After mECD mAb exposure (but not mCCD), AQP4 (green) and CD32B (magenta) colocalize in discrete foci (merged, white). DNA, blue (DAPI). (Scale bars: 20 μm.)

hinge region to FcγR (28, 29). For example, signaling events initiated by antigen-bound IgG interacting with Fc-binding molecules on monocytes and macrophages trigger internalization of the FcγR–IgG–antigen complex and FcγR recycling back to the leukocyte surface (30, 31). Astrocytic and microglial FcγRs have been implicated in CNS disorders beyond adaptive immune functions (18–20). Innate inflammatory events accompanying neurodegeneration are presumed activated in part via FcγR interaction with non-Ig ligands (32). The FcγR-dependent AQP4 internalization we observed in cultures lacking microglia is most readily explained by *cis* interaction between AQP4-bound NMO-IgG Fc and astrocytic FcγRs.

We propose a model (Fig. 7*F*) in which ITAM-dependent signaling through the activating CD64 FcγR gamma subunit initiates AQP4 endocytosis after NMO-IgG binds. Initial CD64 engagement by IgG is a prerequisite for inhibitory FcγR signaling through CD32B (33, 34). CD32B was not phosphorylated when NMO-IgG bound to AQP4 in astrocytes lacking the CD64 gamma subunit. The alpha subunit to which IgG binds is retained in FcγRγ$^{-/-}$ astrocytes (35), but does not suffice to trigger endocytosis of AQP4 tetramers cross-linked by NMO-IgG. Endocytosis of both CD32B and AQP4 from the astrocyte membrane requires the gamma subunit. We suggest that the activating signal (Fig. 7*F, a*) triggers CD32B recruitment and phosphorylation of its ITIM domain (Fig. 7*F, b*), presumably by the same kinase that phosphorylates the gamma subunit's ITAM domain (36). Phosphatases recruited by pCD32B would arrest the signaling cascade initiated by NMO-IgG Fc engaging the CD64 FcγR. After the AQP4:IgG:CD32B immune complex is internalized, AQP4 translocates to the endolysomal pathway for degradation and CD32B is recycled to the astrocytic surface (Fig. 7*F, c*).

CD64 is known to regulate CD32B activation in leukocytes (37). Our study implicates CD64 in regulating a neural protein's surface expression. The data support CD32B being endocytosed with AQP4 and IgG because of its recruitment into a multimolecular immune complex: AQP4:IgG:CD32B. Identification of the signaling pathways through which FcγRs mediate internalization of AQP4 and EAAT2 may reveal new candidate targets for therapeutic prevention or amelioration of NMO relapses.

Materials and Methods

Animal experiments were Mayo Clinic Institutional Animal Care and Use Committee (IACUC)-approved and complied with NIH guidelines. Deidentified NMO patient sera were obtained from the Neuroimmunology Laboratory, Mayo Clinic [approved by the Institutional Review Board (IRB) Biospecimens Subcommittee]. Experimental details [astrocyte cultures (38), antibody sources and specificities, IgG and Fab preparation, immunostaining,

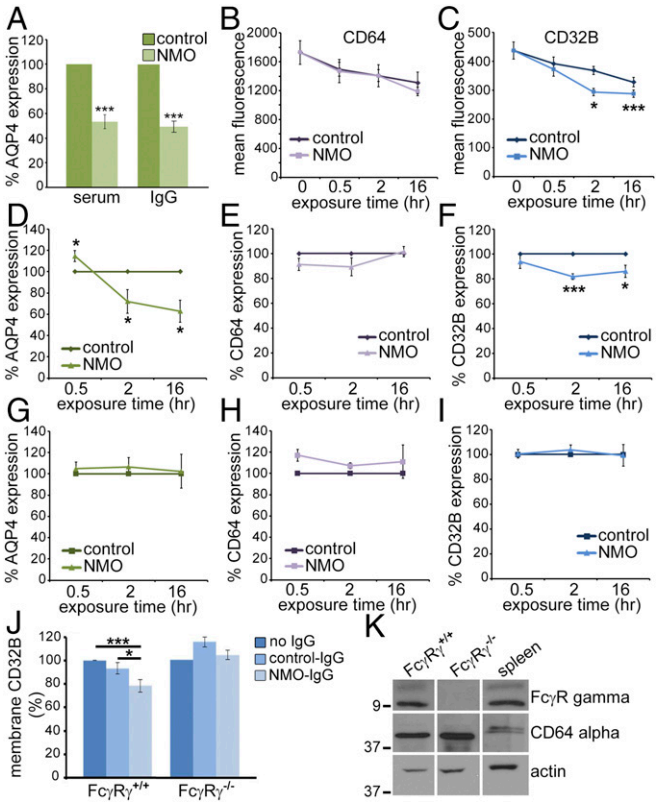

Fig. 6. CD64 FcγR gamma subunit is required for CD32B loss from astrocytic plasma membranes after NMO–IgG–AQP4 interaction. (*A*) Flow cytometric quantitation of surface AQP4 on wild-type astrocytes exposed 16 h to human serum or IgG (***$P < 0.001$). (*B* and *C*) Mean fluorescence (four experiments), surface CD64 (*B*), and CD32B (*C*). CD64 loss not significant ($P = 0.18$ at 16 h). (*C*) CD32B loss was significant after 2 h with NMO serum compared with no serum and control serum (*$P = 0.012$, 0.001). (*D–I*) Relative AQP4, CD64, and CD32B in astrocytes exposed to control or NMO serum ($n = 4$; *D–F*, wild-type; *G–I*, FcγRγ$^{-/-}$). AQP4 in wild-type membranes increased transiently after exposure 30 min to NMO serum (relative to control; *$P = 0.045$); >40% was lost after 2 and 16 h (*D*; *$P = 0.011$). AQP4 in FcγRγ$^{-/-}$ astrocytes did not change significantly (*G*). CD64 alpha subunit did not differ significantly in wild-type or FcγRγ$^{-/-}$ astrocytes (*E* and *H*). CD32B in wild-type membranes was reduced after 2 h NMO serum exposure (*F*; ***$P < 0.001$), remained low at 16 h (*$P < 0.05$), but was not reduced in FcγRγ$^{-/-}$ astrocytes (*I*). (*J*) CD32B on wild-type astrocytes also was reduced (but not on FcγRγ$^{-/-}$ astrocytes) at 2 h with NMO-IgG (*$P < 0.05$, ***$P < 0.001$; compared with nonexposed or control-IgG-exposed cells). (*K*) Relative basal content of CD64 alpha and gamma subunits in wild-type and FcγRγ$^{-/-}$ astrocyte lysates. Gamma was concentrated by immunoprecipitation with subunit-specific IgG. Rat splenic lysate was positive control. Data represent three or more independent experiments.

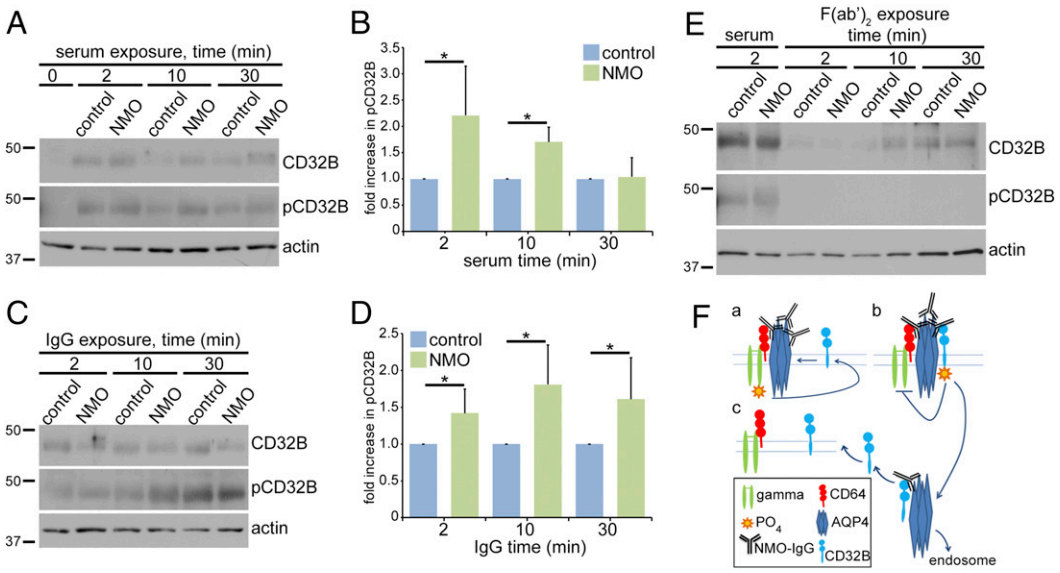

Fig. 7. CD32B phosphorylation induced by NMO IgG products precedes endocytosis of the AQP4:IgG:CD32B complex. Western blot: total CD32B and phosphorylated CD32B (pCD32B) immunoprecipitated with CD32B-IgG from astrocyte lysates after control or NMO serum exposure (*A* and *B*), IgG (*C* and *D*), or F(ab′)$_2$ (*E*). Actin indicates lysate protein content before immunoprecipitation. Quantitation and error bars in *B* and *D* from data of six individual experiments. Exposure to NMO serum or IgG induced CD32B phosphorylation. Control and NMO serum and IgGs, but not F(ab′)$_2$, enhanced CD32B expression. The ratio of pCD32B relative to total CD32B in astrocytes exposed to NMO serum or NMO-IgG compared with astrocytes exposed to control serum or control-IgG [*B*; $*P = 0.01$ (2 min) and 0.0001 (10 min)] [*D*; $*P = 0.01$ (2 min), 0.004 (10 min) and 0.02 (30 min)]. (*F*) Proposed mechanism for astrocytic FcγR interactions with NMO-IgG, preceding AQP4 internalization and degradation (*Discussion*).

IL-6 ELISA, membrane preparations, immunoprecipitations, Western blots (39), flow cytometry (40), and statistical analyses] are in *SI Materials and Methods*.

ACKNOWLEDGMENTS. We thank Jackie Grell for technical assistance, Jim Fryer for characterizing AQP4 mAbs, and Dr. John Henley for reviewing the manuscript. Funding was provided by Mayo Clinic Foundation.

1. Lucchinetti CF, et al. (2014) The pathology of an autoimmune astrocytopathy: Lessons learned from neuromyelitis optica. *Brain Pathol* 24:83–97.
2. Papeix C, et al. (2007) Immunosuppressive therapy is more effective than interferon in neuromyelitis optica. *Mult Scler* 13:256–259.
3. Warabi Y, Matsumoto Y, Hayashi H (2007) Interferon beta-1b exacerbates multiple sclerosis with severe optic nerve and spinal cord demyelination. *J Neurol Sci* 252:57–61.
4. Lennon VA, et al. (2004) A serum autoantibody marker of neuromyelitis optica: Distinction from multiple sclerosis. *Lancet* 364:2106–2112.
5. Lennon VA, Kryzer TJ, Pittock SJ, Verkman AS, Hinson SR (2005) IgG marker of optic-spinal multiple sclerosis binds to the aquaporin-4 water channel. *J Exp Med* 202:473–477.
6. Hinson SR, et al. (2008) Aquaporin-4-binding autoantibodies in patients with neuromyelitis optica impair glutamate transport by down-regulating EAAT2. *J Exp Med* 205:2473–2481.
7. Vincent T, et al. (2008) Functional consequences of neuromyelitis optica-IgG astrocyte interactions on blood-brain barrier permeability and granulocyte recruitment. *J Immunol* 181:5730–5737.
8. Zhang H, Bennett JL, Verkman AS (2011) Ex vivo spinal cord slice model of neuromyelitis optica reveals novel immunopathogenic mechanisms. *Ann Neurol* 70:943–954.
9. Hinson SR, et al. (2012) Molecular outcomes of neuromyelitis optica (NMO)-IgG binding to aquaporin-4 in astrocytes. *Proc Natl Acad Sci USA* 109:1245–1250.
10. Hinson SR, et al. (2007) Pathogenic potential of IgG binding to water channel extracellular domain in neuromyelitis optica. *Neurology* 69:2221–2231.
11. Marignier R, Giraudon P, Vukusic S, Confavreux C, Honnorat J (2010) Anti-aquaporin-4 antibodies in Devic's neuromyelitis optica: Therapeutic implications. *Ther Adv Neurol Disorder* 3:311–321.
12. Takeshita Y, et al. (2016) Effects of neuromyelitis optica-IgG at the blood-brain barrier in vitro. *Neurol Neuroimmunol Neuroinflamm* 4:e311.
13. Howe CL, et al. (2014) Neuromyelitis optica IgG stimulates an immunological response in rat astrocyte cultures. *Glia* 62:692–708.
14. Walker-Caulfield ME, et al. (2015) NFκB signaling drives pro-granulocytic astroglial responses to neuromyelitis optica patient IgG. *J Neuroinflammation* 12:185.
15. Roemer SF, et al. (2007) Pattern-specific loss of aquaporin-4 immunoreactivity distinguishes neuromyelitis optica from multiple sclerosis. *Brain* 130:1194–1205.
16. Takai T, Li M, Sylvestre D, Clynes R, Ravetch JV (1994) FcR γ chain deletion results in pleiotrophic effector cell defects. *Cell* 76:519–529.
17. Kurlander RJ, Ellison DM, Hall J (1984) The blockade of Fc receptor-mediated clearance of immune complexes in vivo by a monoclonal antibody (2.4G2) directed against Fc receptors on murine leukocytes. *J Immunol* 133:855–862.
18. Nitta T, Yagita H, Sato K, Okumura K (1992) Expression of Fc gamma receptors on astroglial cell lines and their role in the central nervous system. *Neurosurgery* 31:83-7-8.
19. Vedeler C, et al. (1994) Fc receptor for IgG (FcR) on rat microglia. *J Neuroimmunol* 49: 19–24.
20. Li YN, et al. (2008) Alterations of Fc gamma receptor I and Toll-like receptor 4 mediate the antiinflammatory actions of microglia and astrocytes after adrenaline-induced blood-brain barrier opening in rats. *J Neurosci Res* 86:3556–3565.
21. Haruki H, et al. (2013) NMO sera down-regulate AQP4 in human astrocyte and induce cytotoxicity independent of complement. *J Neurol Sci* 331:136–144.
22. Ghazizadeh S, Fleit HB (1994) Tyrosine phosphorylation provides an obligatory early signal for Fc gamma RII-mediated endocytosis in the monocytic cell line THP-1. *J Immunol* 152:30–41.
23. Içöz S, et al. (2010) Enhanced IL-6 production in aquaporin-4 antibody positive neuromyelitis optica patients. *Int J Neurosci* 120:71–75.
24. Uzawa A, et al. (2010) Cytokine and chemokine profiles in neuromyelitis optica: Significance of interleukin-6. *Mult Scler* 16:1443–1452.
25. Araki M, et al. (2014) Efficacy of the anti-IL-6 receptor antibody tocilizumab in neuromyelitis optica: A pilot study. *Neurology* 82:1302–1306.
26. Dhodapkar KM, et al. (2007) Selective blockade of the inhibitory Fcgamma receptor (FcgammaRIIB) in human dendritic cells and monocytes induces a type I interferon response program. *J Exp Med* 204:1359–1369.
27. Geis C, et al. (2015) The intrinsic pathogenic role of autoantibodies to aquaporin 4 mediating spinal cord disease in a rat passive-transfer model. *Exp Neurol* 265:8–21.
28. Jefferis R, Lund J (2002) Interaction sites on human IgG-Fc for FcgammaR: Current models. *Immunol Lett* 82:57–65.
29. Chavele K-M, et al. (2010) Mannose receptor interacts with Fc receptors and is critical for the development of crescentic glomerulonephritis in mice. *J Clin Invest* 120:1469–1478.
30. Harrison PT, Davis W, Norman JC, Hockaday AR, Allen JM (1994) Binding of monomeric immunoglobulin G triggers Fc gamma RI-mediated endocytosis. *J Biol Chem* 269:24396–24402.
31. Jaumouillé V, et al. (2014) Actin cytoskeleton reorganization by Syk regulates Fcγ receptor responsiveness by increasing its lateral mobility and clustering. *Dev Cell* 29:534–546.
32. Okun E, Mattson MP, Arumugam TV (2010) Involvement of Fc receptors in disorders of the central nervous system. *Neuromolecular Med* 12:164–178.
33. Daëron M, Jaeger S, Du Pasquier L, Vivier E (2008) Immunoreceptor tyrosine-based inhibition motifs: A quest in the past and future. *Immunol Rev* 224:11–43.
34. Smith KGC, Clatworthy MR (2010) FcgammaRIIB in autoimmunity and infection: Evolutionary and therapeutic implications. *Nat Rev Immunol* 10:328–343.
35. van Vugt MJ, et al. (1996) FcR gamma-chain is essential for both surface expression and function of human Fc gamma RI (CD64) in vivo. *Blood* 87:3593–3599.
36. Malbec O, et al. (1998) Fc epsilon receptor I-associated lyn-dependent phosphorylation of Fc gamma receptor IIB during negative regulation of mast cell activation. *J Immunol* 160:1647–1658.
37. Altrichter J, et al. (1995) Phosphatidylinositol hydrolysis and an increase in Ca2+ concentration in the signal-transduction process triggered by murine Fc gamma RIII are not required for protein kinase C translocation. *Eur J Biochem* 228:587–595.
38. McCarthy KD, de Vellis J (1978) Alpah-adrenergic receptor modulation of beta-adrenergic, adenosine and prostaglandin E1 increased adenosine 3′:5′-cyclic monophosphate levels in primary cultures of glia. *J Cyclic Nucleotide Res* 4:15–26.
39. Neely JD, Christensen BM, Nielsen S, Agre P (1999) Heterotetrameric composition of aquaporin-4 water channels. *Biochemistry* 38:11156–11163.
40. Clift IC, Bamidele AO, Rodriguez-Ramirez C, Kremer KN, Hedin KE (2014) β-Arrestin1 and distinct CXCR4 structures are required for stromal derived factor-1 to downregulate CXCR4 cell-surface levels in neuroblastoma. *Mol Pharmacol* 85:542–552.